Scientia Iranica B (2017) 24(6), 2963–2976

SCIENTIA IRANICA

Sharif University of Technology
Scientia Iranica
Transactions B: Mechanical Engineering
www.scientiairanica.com

Research Note

Influence of printed circuit board thickness in wave soldering

M.S. Abdul Aziz[a,*], M.Z. Abdullah[b], C.Y. Khor[c], I.A. Azid[d], A. Jalar[e] and F. Che Ani[e,f]

a. *School of Mechanical Engineering, Universiti Sains Malaysia, 14300 Nibong Tebal, Penang, Malaysia.*
b. *School of Aerospace Engineering, Universiti Sains Malaysia, 14300 Nibong Tebal, Penang, Malaysia.*
c. *Faculty of Engineering Technology (FETech), Universiti Malaysia Perlis (UniMAP), Level 1, Block S2, UniCITI Alam Campus, Sungai Chuchuh, 02100, Padang Besar, Perlis, Malaysia.*
d. *Mechanical Section, Universiti Kuala Lumpur Malaysian Spanish Institute, Kulim Hi-Tech Park, 09000 Kulim, Kedah, Malaysia.*
e. *Institute of Microengineering and Nanoelectronics, University Kebangsaan Malaysia, 43600 Bangi, Selangor, Malaysia.*
f. *Jabil Circuit Sdn. Bhd., Bayan Lepas Industrial Park, 11900, Bayan Lepas, Penang, Malaysia.*

Received 20 October 2015; received in revised form 29 June 2016; accepted 21 November 2016

KEYWORDS
Printed Circuit Board (PCB);
Wave soldering;
Thermal fluid-structure interaction;
Thermal stress;
Displacement.

Abstract. This paper presents a thermal Fluid-Structure Interaction (FSI) study of Printed Circuito Bards (PCBs) during wave soldering. The influences of PCB thickness on displacement, stress, and temperature distribution are the foci of this study. Five PCB thicknesses (i.e., 0.6, 1.0, 1.6, 2.4, and 3.1 mm) are considered. The paper focuses on a simple PCB with a single hole and is constructed in a three-dimensional model. The thermal FSI of the PCB is solved by fluid (FLUENT) and structure (ABAQUS) solvers that are connected using the mesh-based parallel code coupling interface method. Molten solder advancement is tracked using volume-of-fluid technique in the thermal fluid analysis. ABAQUS solves PCB displacement, von Mises stress, and temperature distributions when high solder temperature is encountered during wave soldering. The correlations of PCB thickness with displacement, von Mises stress, temperature distribution, and molten solder filling time are studied. Results reveal that an increase in PCB thickness yields a linear correlation with solder filling time. Temperature distribution, von Mises stress, and displacement of PCB exhibit polynomial behavior to PCB thickness. A laboratory-scale two-way wave-soldering machine is also used to measure PCB temperature during wave soldering. The predicted temperature of PCB is substantiated by the experimental results.

1. Introduction

Printed Circuit Boards (PCB) play an important role in electronic devices and components. PCBs are fabricated from different organic materials that are printed with the circuits such as polyimide, FR-1, FR-2, FR-4, bismaleimide, and cyanate ester. The complexity of PCBs can be classified into single-sided, double-sided, and multi-layered. Printed circuits provide power and connect the components and Integrated Circuit (IC) package. Moreover, PCBs function as carriers of components and IC packages. In assembly process, the PCB experiences temperature variations in different assembly stages, such as during reflow and wave soldering. Typically, the temperature at reflow and

*. *Corresponding author. Tel.: +60165584438*
E-mail address: msharizal@usm.my (M.S. Abdul Aziz)

doi: 10.24200/sci.2017.4311

wave soldering is around 240°C to 250°C. During these processes, PCB temperature increases and decreases at each stage. These temperature variations may induce PCB warpage, which is also recognized as out-of-plane displacement [1]. The coefficient of thermal expansion mismatch among the materials results in PCB warpage. PCB warpage is a concern not only for board transfer during automated assembly, but also for the performance of the final assembly because it may lead to severe solder joint failures.

On the one hand, multifarious studies have been conducted to investigate PCB warpage. Nonetheless, most of these studies concentrated on the solder reflow process through experiments [2] and simulations [3]. In literature, many researchers used the Finite-Element Method (FEM) [3-5] to investigate the PCB and substrate warpage. However, an investigation of PCB deformation using thermal Fluid-Structure Interaction (FSI) has yet to be reported. Nonetheless, warpage investigations have been extended to IC packages [6], such as flip-chip Ball Grid Array (BGA) packages. Ding et al. [7] studied the parametric effects of materials, geometry, and process of PCB assembly during reflow. Taguchi and full-factorial design of experiments were used to optimize parameters and minimize warpage. Shadow Moir [8] is a renowned method used in experimental work to measure PCB warpage. The deflection of PCB is evaluated through captured grating by the system. However, in simulation modeling analysis, most of the warpages and solder joints [9] were predicted through FEM, which only involves the structural solver. Temperature endurance to PCB depends on the input setting.

On the other hand, only a few investigators have conducted a study on wave soldering. Polsky et al. [10] investigated PCB warpage caused by infrared reflow and wave soldering. Two PCB layouts were used to study thermally induced deflection. They observed that both PCBs experienced large deflection (bowl-like shape) in wave soldering, an effect that is attributed to the presence of larger through-thickness thermal gradients. The PCB deflection was evaluated by using a shadow Moire pattern. To minimize warpage, Johnson [11] reported the advantages of a pallet during wave soldering. The pallet exposes the particular PCB region (soldering area) to the solder wave, which can minimize PCB warpage during wave soldering. During wave soldering, when the pallet absorbs heat from the solder wave, only a portion of heat is absorbed by PCB. This method can minimize PCB warpage, but the pallet is warped or twisted when it is exposed to high temperature. The pallet design and material used are important to solve this problem. Moreover, Hutapea and Grenestedt [12] reported that the wavy copper trace design of PCBs can minimize 40% to 60% of warpage compared with a typical straight copper trace.

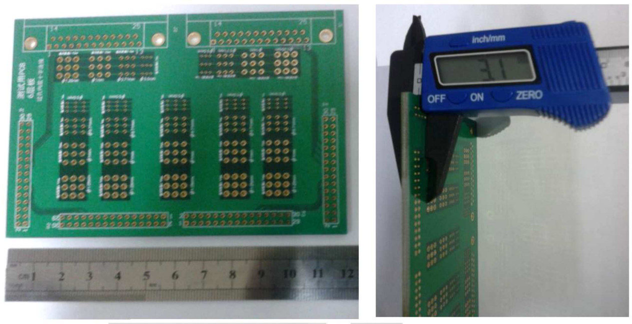

(a) Front view (b) Side view

Figure 1. PCB testboard with 3.1 mm thickness.

Studies on PCB warpage during soldering reflow using FEM have been extensively reported in literature. However, the simulation analysis of PCB warpage during wave soldering is rarely reported. Therefore, this study investigated PCB warpage during wave soldering. In industry, a typical wave soldering process consists of different zones: fluxing, preheating, soldering, and cooling. The settings of wave soldering machines may differ from diverse PCB specifications, such as board size, thickness, hole size, and component layout. For example, these elements may influence the settings of preheating and solder temperature. The filling of molten solder, temperature distribution, and thermal stress are also difficult to visualize in the experiment. The application of simulation tools is advantageous to tackle these problems. Therefore, only simplified PCB with a single hole was considered in investigating the filling process, temperature distribution, displacement, and thermal stress. The thickness of the PCB used (i.e., 0.6, 1.0, 1.6, 2.4, and 3.1 mm) in industry depends on the PCB design area (Table 1). The example of a PCB with thickness of 3.1 mm is shown in Figure 1. Different PCB thicknesses with a constant PCB size were considered, and the focus was directed on the PCB hole region. Thermal FSI analysis was conducted using Mesh-based Parallel Code Coupling Interface (MpCCI) to connect fluid and structural solvers. Moreover, the experiment was performed using a laboratory-scale two-way wave-soldering machine. The measured PCB temperature was compared with the simulation results.

2. Methodology

The basic concept of the thermal FSI analysis is the use of MpCCI software for transferring numerical data simultaneously. This coupling technique connects both fluid and structural solvers that operate in real time. Figure 2 illustrates the overview of MpCCI thermal FSI analysis in the current study. Molten solder flow is modelled by FLUENT. During the filling process, the PCB experiences the temperature of molten solder.

Table 1. Minimum board thickness requirements.

Longest board dimension (length or width)	Minimum board thickness
Longest board dimension $\leq$ 12.5 cm (4.92″) Area $\leq$ 75 cm^2 (11.63″^{2})	0.6 mm (0.024″)
Longest board dimension $\leq$ 17.0 cm (6.69″) Area $\leq$ 150 cm^2 (23.25″^{2})	1.0 mm (0.040″)
Longest board dimension $\leq$ 25.0 cm (9.84″) Area $\leq$ 300 cm^2 (46.5″^{2})	1.6 mm (0.062″)
Longest board dimension $\leq$ 40 cm (15.75″) Area $\leq$ 900 cm^2 (139.5″^{2})	2.4 mm (0.093″)
Longest board dimension $>$ 40 cm (15.75″) Area $>$ 900 cm^2 (139.5″^{2})	3.1 mm (0.120″)

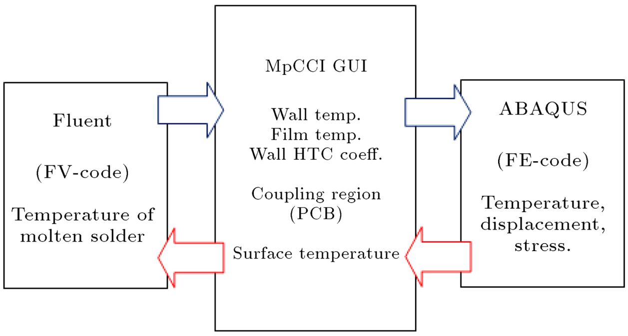

Figure 2. Overview of MpCCI thermal-FSI.

Temperature data are transferred to the ABAQUS for structural analysis. Once the ABAQUS receives the data, it solves the thermal-induced displacement and stress of the PCB. The ABAQUS then sends the response to the FLUENT for a complete cycle.

2.1. Fluid flow modeling

The filling of molten solder is driven by capillary action in wave soldering. The fluid motion is described by continuity and momentum equations [13]. The fluid temperature is expressed by an energy equation. In this simulation, the Volume-Of-Fluid (VOF) method was applied to track the filling of molten solder at the PCB hole. VOF method locates and distributes the liquid phase by attaching each cell to the computational elements. F is the volume fraction of cells occupied by the liquid phase. Thus, the value of $F = 1$ in a cell contains only molten solder (63Sn37Pb). The value of $F = 0$ in grids is the void formed in the molten solder. A value of $1 < F < 0$ in the "interface" cells is referred to as the melt front of the molten solder. Thus, the molten solder surface was assumed to be on the volume fraction of 0.5. This fraction was used to evaluate the filling level of the molten solder. It was also used to evaluate liquid phase in various CFD applications [13-16]. Wetting the PCB surface is important during wave soldering. To form a solder joint (Figure 3) in wave soldering, all the parts must be solderable. Metal surfaces must be wetted by soldering. Wetting grade can be measured by the wetting angle according to Young's equation. Capillary behavior is a result of the pressure differences between two sides of a curved liquid surface. Figure 4 shows the capillary action during wave soldering.

In a simulation analysis, the PCB and fluid domain of wave soldering were created by GAMBIT

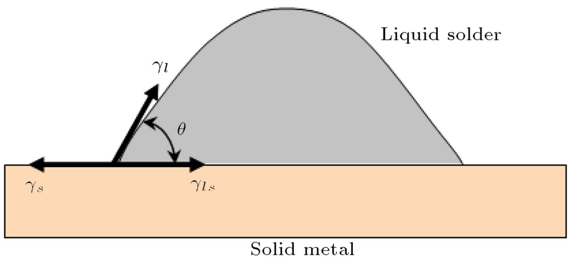

Figure 3. Surface tension between solid surface and liquid solder.

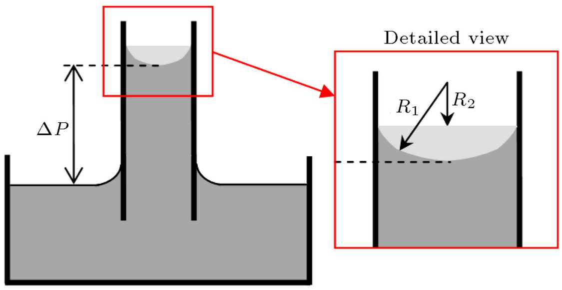

Figure 4. Capillary action of wave soldering.

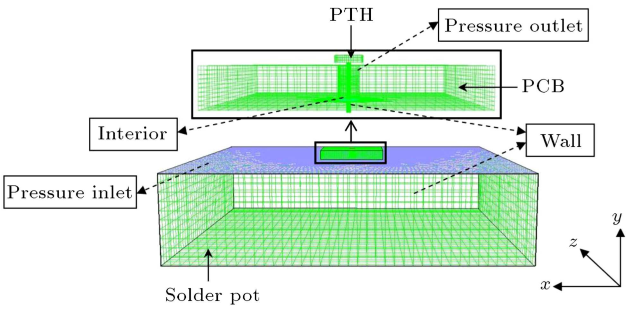

Figure 5. Meshed model and boundary conditions of the simulation model.

Table 2. Dimensions of PCB.

Parameter	Dimension (mm)
PCB (length × width)	16 × 16
PCB thickness	0.6; 1.0; 1.6; 2.4; 3.1
PCB hole (diameter)	1.5

Table 3. Solder material and thermal properties.

Parameter	Value
Viscosity (Pa.s)	0.0018
Density (kg/m^3)	8510
Specific heat capacity, Cp (j/kg-k)	183
Thermal conductivity (W/m-k)	53

software. The computational domain was meshed with 356,251 tetrahedral elements (Figure 5).

The PCB is defined as a coupling region for the FLUENT and ABAQUS solvers. The surfaces of the domain and PCB are defined as the wall boundaries. Wall temperature, film temperature, and heat transfer coefficient of the wall were transferred from the FLUENT to ABAQUS during the simulation. However, the surface temperature of PCB was sent to the FLUENT from ABAQUS. Table 2 summarizes the detailed dimensions of the PCB, and Table 3 lists the solder material properties. Similar simulation settings were adopted from Abdul Aziz et al. [17] for the current thermal FSI analysis.

2.2. *Structural modeling*

A simplified multi-layered PCB model was subjected to wave soldering, and the thermal-induced displacement and stress distribution were investigated. Structural analysis was conducted using ABAQUS software. The calculations of the displacement and stress were dependent on the temperature of the molten solder (FLUENT). The PCB model was created according to the size, position, and coordinate of the FLUENT model (Figure 6(a)) to allow the coupling between fluid and structural solvers. Carrier jaws held the PCB during wave soldering. Thus, a fixed boundary was set on the two sides of the PCB (Figure 6(b)). The PCB

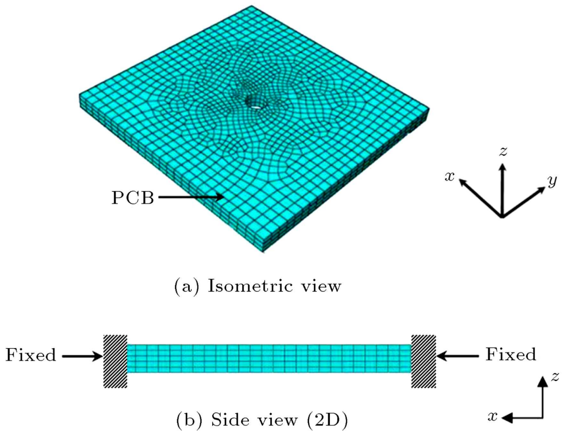

Figure 6. (a) Meshed model of simplified PCB. (b) Fixed boundary condition.

Table 4. Thermal and mechanical properties of FR-4 PCB [18-20].

Parameter	Value
Density (kg/m^3)	1700
Thermal conductivity (W/mK)	0.2
Specific heat capacitance J/(kgK)	920
Young's modulus (MPa)	18200
CTE (ppm/K)	15
Poisson's ratio	0.25
Yield strength (MPa)	65-70

model was meshed with hexahedral elements (C3D8T-8-node trilinear displacement and temperature), and the PCB material was modeled as a linear isotropic material [18-20] in the ABAQUS. Table 4 summarizes the thermal and mechanical properties of PCBs.

2.3. *Mesh convergence study*

Mesh convergence study was carried out to determine the appropriate number of elements before the simulation analysis. Figure 7 shows the displacement versus the position for various numbers of elements. Displacement of the PCB was examined for different meshes. The test discovered that the displacement of the PCB is converged in Mesh 5 and Mesh 6. This phenomenon is evidently observed in Figure 7, whereas both Mesh 5 and Mesh 6 have almost an identical trend and Mesh 5 has the smallest deviation (in Table 5) when compared with Mesh 6. Thus, the number of elements between 2776 and 3156 was considered in the current simulation analysis.

3. Experimental procedure

Figure 8 illustrates the laboratory-scale two-way leaded/lead-free wave-soldering machine. The experiment was performed to substantiate the simulation results. In the experiment, the thermal stress and

Table 5. Displacement, computing time of different numbers of elements for the convergence test.

Mesh	1	2	3	4	5	6
Elements	1628	1878	2142	2413	**2776**	3156
Displacement (mm), at position 0.8 mm	2.01e-6	3.56e-6	5.59e-6	7.56e-6	**1.06e-5**	1.11e-5
Deviation from Mesh 6	9.09e-6	7.54e-6	5.51e-6	3.54e-6	**5.00e-7**	0.00
Computing time (hours)	54	60	65	70	**74**	78

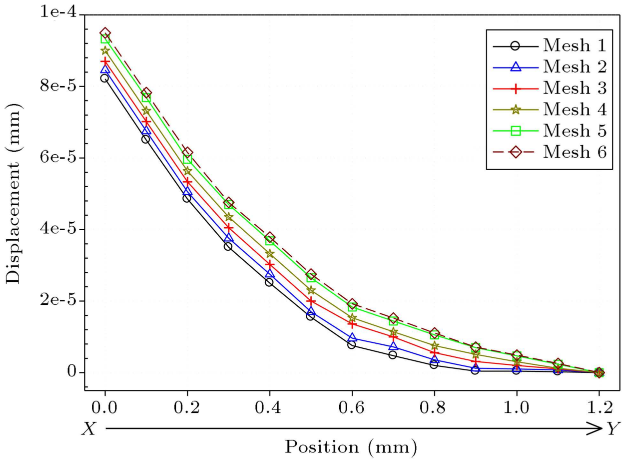

Figure 7. Displacement versus position X-Y for various numbers of elements.

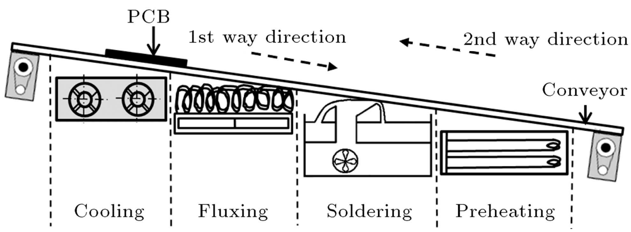

Figure 8. Leaded/lead free wave soldering machine.

displacement of PCB were difficult to visualize during wave soldering. The visualization process may also require costly equipment and setup. In the present experiment, the data acquisition (DAQ) device using a PC-based approach was utilized in a high-performance monitoring and control system to record the temperature of molten solder during wave soldering. K-type thermocouples were attached to the top and bottom of the single circular pin connector to monitor the temperature profiles during soldering (Figure 9). The wave-soldering machine consists of fluxing, preheating, soldering, and cooling zones. Table 6 presents the operation of the two-way wave-soldering machine. In the first way, the PCB passes through the fluxing tank to the preheating zone. At this stage, the soldering zone is not activated. After preheating, the solder fountain is generated once the conveyor moves in the reverse direction. Next, the PCB undergoes wave soldering. In the experiment, the solder pot was inserted with 55 kg Sn63Pb37 and set to 523.15 K (250°C).

Table 6. Operation of two-way wave soldering machine.

Zone	Fluxing	Preheating	Soldering	Cooling
1st way	Active zone	Active zone	—	—
2nd way	—	—	Active zone	Active zone

Prior to soldering, the speed of the solder pump was adjusted to ensure a particularly smooth and stable solder. The PCB attached to thermocouples then passes through the molten solder. The temperature subjected to the pin was recorded by DAQ during wave soldering. The measured experimental temperature was compared with the simulation result.

4. Results and discussion

4.1. Experimental validation

Figure 10 shows the temperature profile of the top and bottom PCB recorded in the experiment. The temperature increases drastically from the preheating zone to the soldering zone, when the PCB passes through the solder pot. At this stage, the molten solder fills the PCB hole through capillary action. Subsequently, the temperature of the bottom PCB decreases gradually at the cooling zone. However, no significant changes are observed in the temperature of the top PCB, which gradually increases along the process. From the experiment, the temperature profile of PCB indicates that PCB experiences critical temperature variations in different zones during wave soldering. The measured temperatures of PCB (top and bottom) were compared with the predicted simulation results. Figure 11 illustrates the comparison of the predicted simulation and experimental results. In this figure, the predicted results are substantiated by the experimental results for both temperatures. The predicted temperature is important for accuracy in the structural analysis. Thus, the results demonstrate the capability of the simulation technique to solve the problems in wave soldering.

4.2. Overview of thermal FSI at PCB thickness = 2.4 mm

Figure 12 depicts the solder profile and von Mises stress during the molten solder filling process. Molten solder in the PCB hole is driven by capillary action

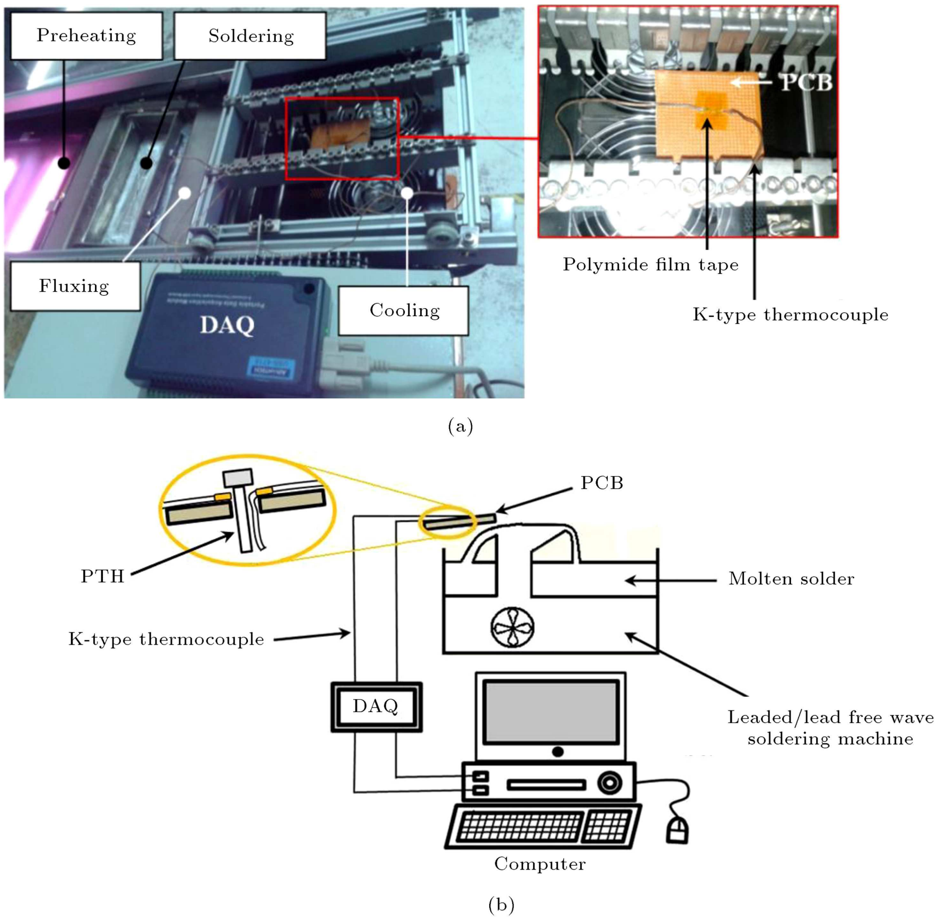

Figure 9. (a) Actual and (b) schematic illustration of experimental setup.

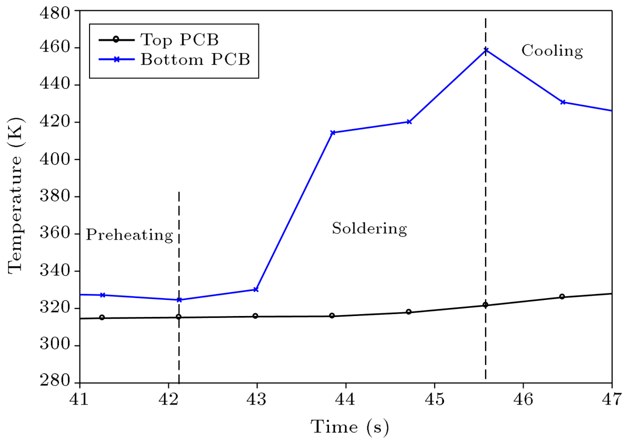

Figure 10. Temperature profile at soldering zone.

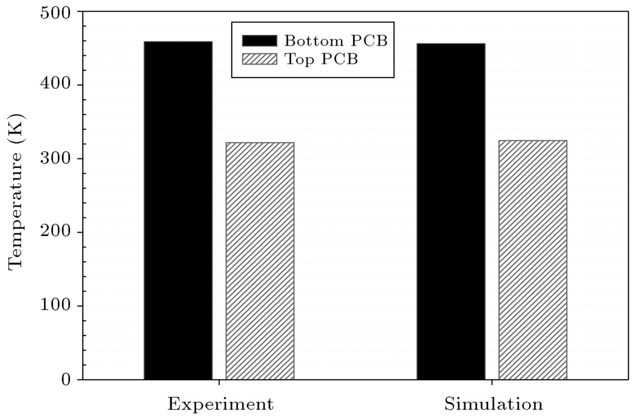

Figure 11. Comparison of bottom and top PCB temperatures between experiment and simulation.

to fill the space in vertical direction. As the PCB experiences the temperature of the molten solder, the structure of the PCB hole endures thermal stress. At 0.38 filling time, the highest stress is observed at the bottom region of the PCB hole. This situation is attributed to the high molten solder temperature and the direct contact between the PCB bottom surface and the molten solder. In Figure 12, the von Mises stress profile of the PCB hole corresponds to the solder filling level. The increase in filling level increases the stress profile because of the conduction of the PCB to the solder temperature. Interestingly, the stress profile shows a bell shape because the bottom region of the PCB experienced higher temperature than the top region of the PCB. This phenomenon clearly indicates that the temperature of molten solder induces stress to the PCB structure.

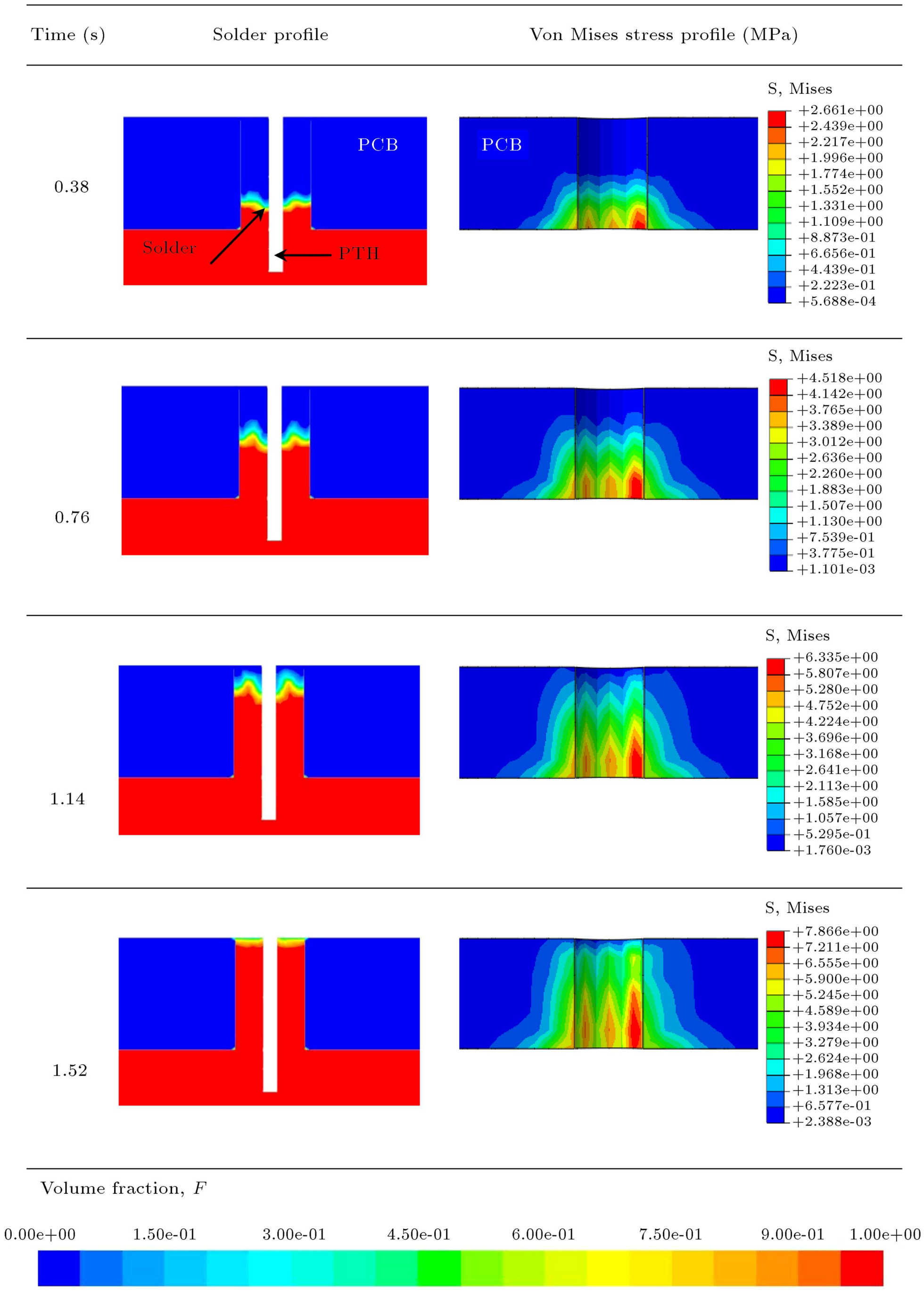

Figure 12. Overview of thermal FSI.

4.3. Profile at 50%, 75%, and 100% filling level for different PCB thicknesses

Figure 13 shows the cross-section of the PCB. A line between two points (A-B, C-D, and X-Y) was used to evaluate the PCB displacement, thermal stress, and filling level for different PCB thicknesses. Figure 14 shows the filling profile of molten solder for different PCB thicknesses, i.e. 0.6, 1.0, 1.6, 2.4, and 3.1 mm. The increase in PCB thickness increases the filling time. The results disclose that filling time is linearly correlated with the PCB thickness (Figure 15). In actual wave soldering, 100% filling is desirable while a minimum 75% vertical filling of the PCB hole is acceptable; otherwise, there will be defects according to the Acceptability of Electronic Assemblies standards [21]. Thus, 50% and 75% filling levels were used for comparison. The molten solder showed uniform and symmetric profiles at 50% and 75% for a thin PCB (0.6 mm). In Figure 14, the increase in PCB thickness causes the uneven molten solder profile in the filling process. A convex molten solder profile was observed at the intermediate space (between the PCB hole surface

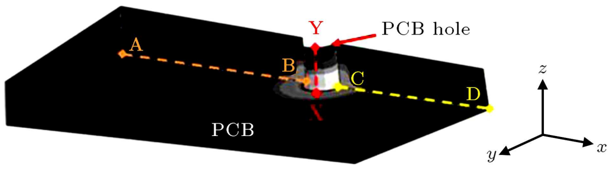

Figure 13. Points A-B, C-D, and X-Y.

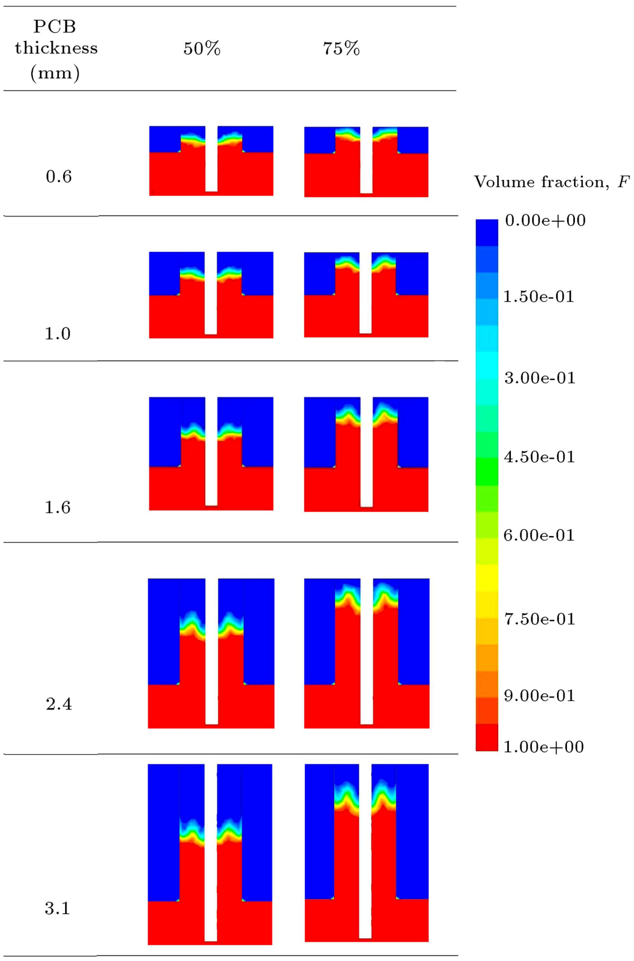

Figure 14. Profile at 50% and 75% filling level.

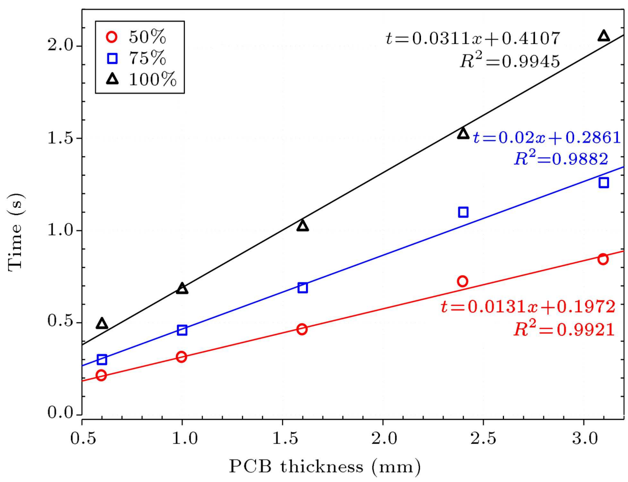

Figure 15. Time at 50%, 75%, and 100% filling.

and pin). Moreover, the meniscus was found in the region of the hole surface of a thick PCB (3.1 mm). This situation may be attributed to the variation in surface tension of the PCB hole and the pin. The pin offset [17], shape [22], and diameter [23] also caused an unbalanced filling profile of the PCB hole. An uneven molten solder profile sometimes induces an incomplete filling or void of the Pin Through Hole (PTH) joint, reducing the strength of the solder joint.

4.4. Temperature distribution within PCB hole at 50% and 100% filling

The temperature distribution of the PCB at various thicknesses was investigated. Figure 16 presents the temperature distribution at 0.6 and 3.1 mm PCB thickness. In the figure, high temperature is observed at the bottom region of the PCB for each case because the bottom PCB is in direct contact with the molten solder during the process. A similar phenomenon is observed at the PCB hole at 50% filling level, where the temperature is higher in the lower region as illustrated in the detailed view. The PCB hole surface conducts heat once it makes contact with the molten solder. Thus, the upper region of the PCB hole is exposed to the temperature of the molten solder. Figure 17 plots the temperature distribution of the PCB. The temperature at point Y is lower than that of point X. Figure 15 shows that 100% filling of the PCB hole only took 2.1 s for a thick PCB (3.1 mm). This finding indicates that wave soldering is a considerably fast and short process.

Therefore, the inner PCB structure experiences lower temperature distribution than the outer surface of the PCB (Figure 16). The temperature distribution may differ for diverse PCBs. Different process settings may be required for different PCB specifications in industry. Temperature difference (ΔT) between the top and bottom PCB was evaluated for each case, as depicted in Figure 18. ΔT increases gradually and corresponds to the PCB thickness, indicating that thick PCB causes a larger temperature difference in the soldering zone. Polsky et al. [10] observed a similar phenomenon in their experiments. They noted that the temperature difference between the top and bottom PCB during wave soldering (approximately 42°C) is higher during the infrared reflow process ($\sim$ 28°C).

4.5. PCB displacement at 100% filling

In the PCB assembly process, the PCB undergoes the solder reflow process for surface mount components, such as BGA packages and leadless components. Afterward, wave soldering is conducted to allow the PCB to assemble the PTH component. Typically, PTH components comprise resistors, capacitors, and pin connectors. The deformed PCB may weaken the inner circuit and influence the solder joint reliability.

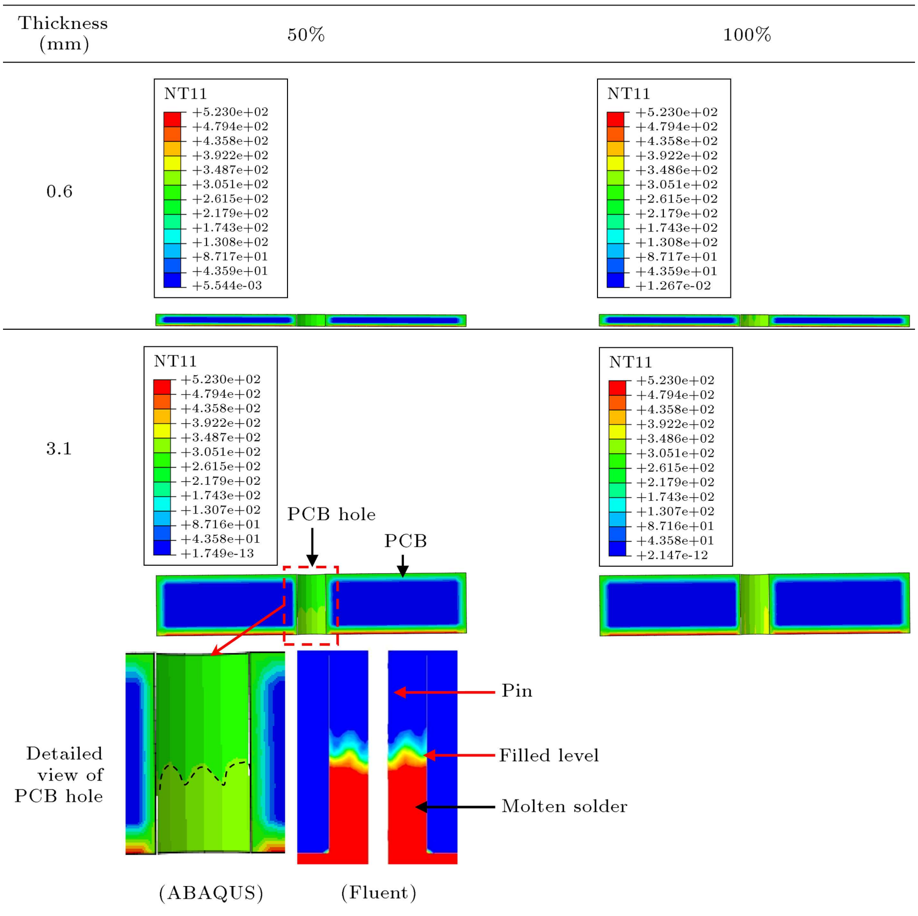

Figure 16. Temperature distribution within PCB hole at 50% and 100% filling level.

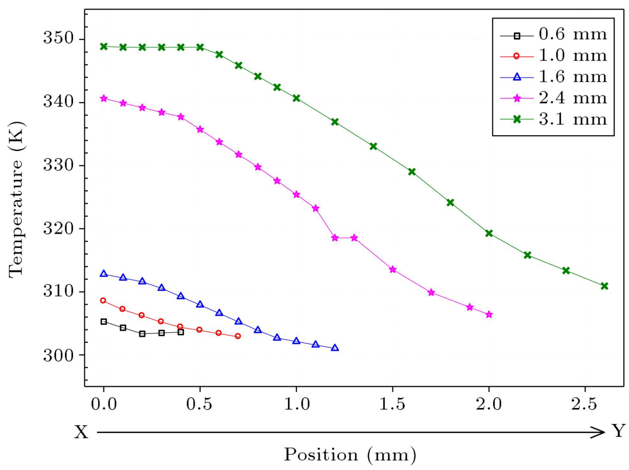

Figure 17. Temperature distribution at different PCB thicknesses.

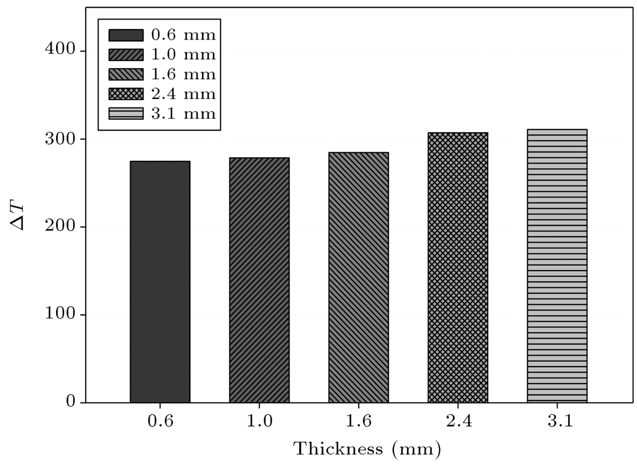

Figure 18. ΔT (K) at different PCB thicknesses, $|T_x - T_y| = \Delta T$.

Figure 19 shows the displacement contour of 0.6 and 3.1 mm PCB thicknesses. The displacement is concentrated around the PCB hole region. The bottom region of the PCB hole has the highest displacement compared with the neighboring regions. The displacement profile for each PCB thickness corresponds to the temperature distribution. The temperature at X-Y (position X-Y; see Figure 13) decreases from points X to Y. Similarly, the displacement of the PCB hole decreases from points X to Y (Figure 20). The displacement at point X behaves in a polynomial manner to increase PCB thickness (Figure 21). Figure 22 presents the displace-

Thickness (mm)	Displacement (mm)
0.6	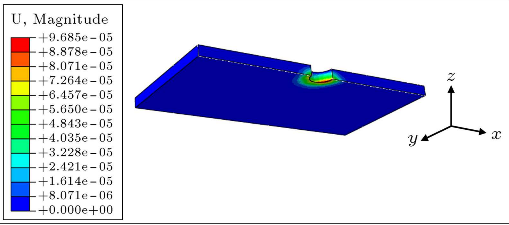
3.1	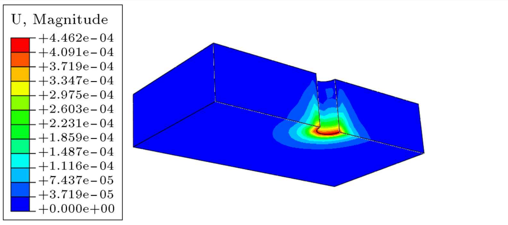

Figure 19. Displacement contour around the PCB hole.

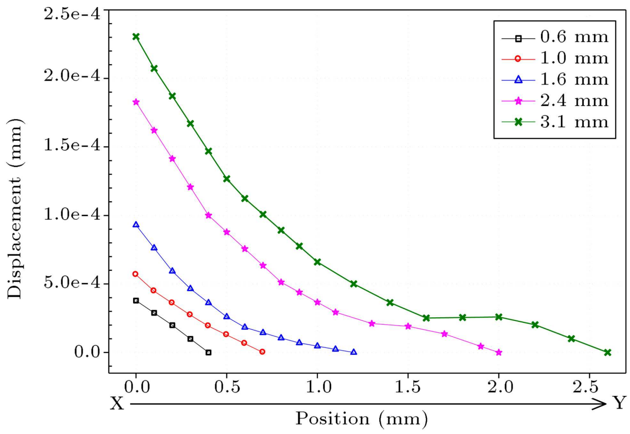

Figure 20. Displacement along X-Y at different thicknesses.

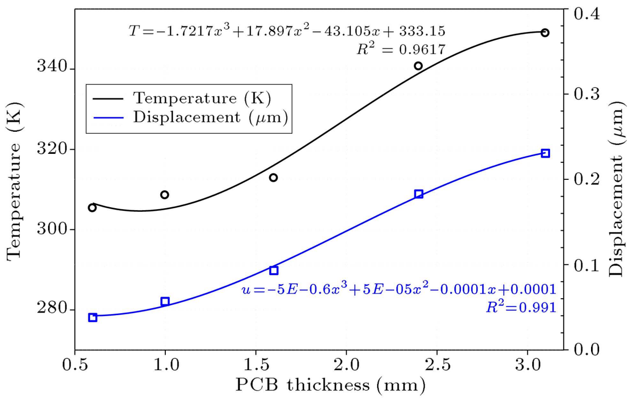

Figure 21. Correlation of PCB thickness with temperature and displacement (at point X).

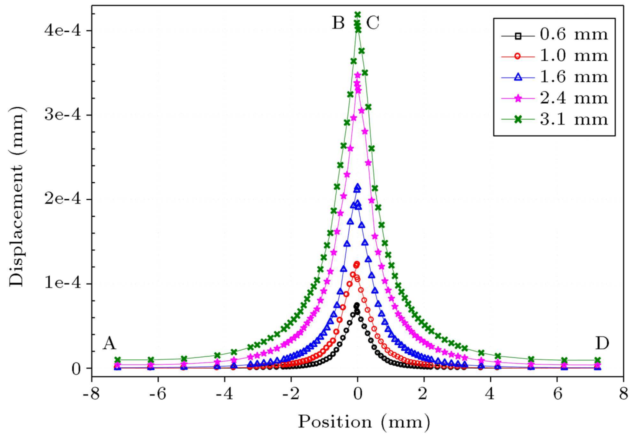

Figure 22. Displacement along A-B and C-D at different thicknesses.

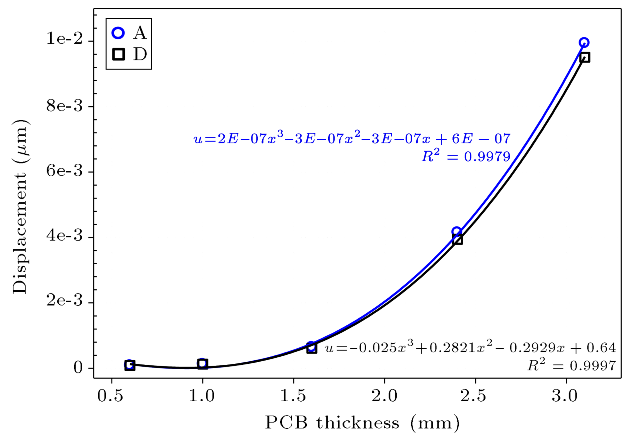

(a) At points A and D

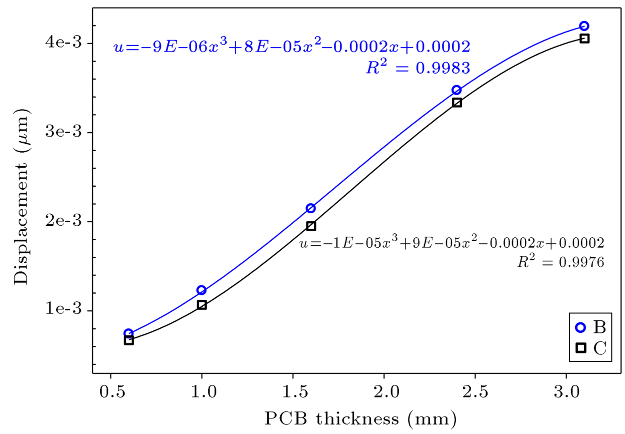

(b) At points B and C

Figure 23. Correlation of PCB thickness with displacement.

ment (lines A-B and C-D; see Figure 13) for different PCB thicknesses. Results reveal that displacement at positions A-D and B-C exhibits polynomial behavior with the change in PCB thickness (Figure 23). The plots indicate that displacement can cause the PCB to deform in a convex shape. Thick PCB (3.1 mm) experiences greater displacement among all the cases because of the large temperature difference between the top and bottom of the PCB during wave soldering [10]. To minimize PCB displacement during wave soldering, the PCB carrier [11] can be used to increase the rigidity of the large PCB. Thus, the proper setting of preheating time and solder temperature is important to reduce PCB displacement.

4.6. Von Mises stress on PCB at 100% filling

Figure 12 shows that von Mises stress varies with molten solder filling time for 2.4 mm PCB thickness (see Section 4.2). Therefore, only the von Mises stress profile at 100% filling was selected for comparison. Figure 24 shows the stress distribution of various PCB thicknesses. The stress of the PCB hole is distributed like a bell, with a larger stress region at the bottom PCB hole than one at the top region. Section 4.2 presents the discussion on the bell-shaped stress distribution. High temperature in the molten solder contributes to the thermal stress of the PCB structure. The simulation results reveal that 3.1 mm PCB thickness is exposed to the highest stress on the PCB hole compared with other thicknesses. As the filling time increases, the PCB hole conducts more heat, increasing the stress on the structure. Figure 25 presents the maximum von Mises stress of the PCB hole. The maximum stress for 3.1 mm PCB thickness is at 8.8 MPa. The concentrated stress in the PCB hole may weaken the solder joint, causing undesired defects such as open solder joint [3] in subsequent manufacturing processes.

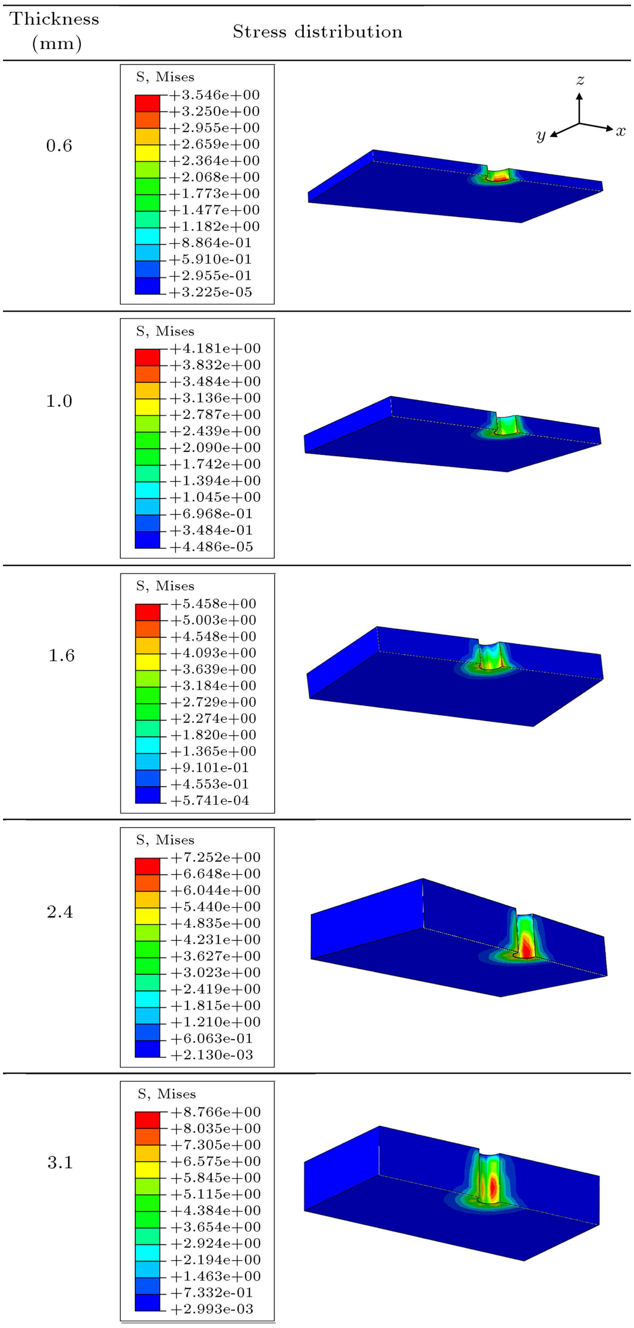

Figure 24. Stress (MPa) distribution along PCB.

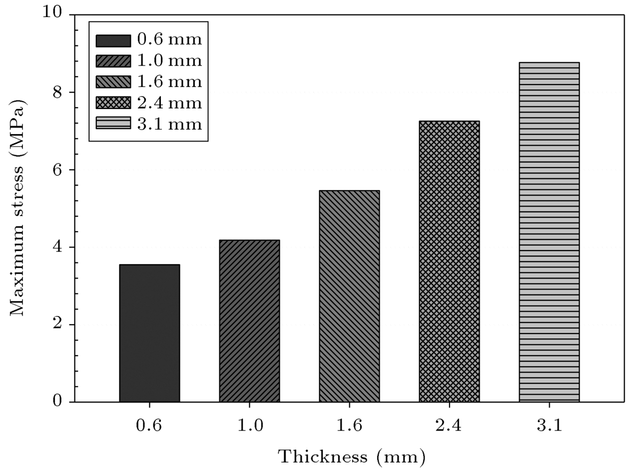

Figure 25. Maximum von Mises stress at different PCB thicknesses.

5. Conclusions

A study on the effects of PCB thickness on PCB displacement, von Mises stress, temperature profile, molten solder profile, and filling time was conducted. A range of PCB thickness was considered according to the requirement of PCB thickness in industry. Thermal FSI analysis was performed using FLUENT-MpCCI-ABAQUS software. The simulation results reveal that an increase in the PCB thickness increases the molten solder filling time in linear correlation. Displacement, von Mises stress, and temperature difference exhibit polynomial behavior to PCB thickness and cause uneven molten solder profiles. The convex profile was observed in the intermediate space between the hole surface and the pin. Displacement and von Mises stress profiles of the PCB hole distributed in a bell shape were identified in all cases. PCB thickness at 3.1 mm experienced the highest displacement (0.004 mm) at the hole edge and von Mises stress (8.8 MPa) on the inner PCB hole surface. This situation was attributed to the longer filling time of PCB heat conduction.

A wave soldering experiment was also performed to measure the temperature of the top and bottom PCB. The PCB temperatures were verified by predicting the simulation results. This study is expected to provide engineers and researchers with a better understanding of and insight into wave soldering. In future studies, the effects of PCB warpage on the solder joint of surface mount components during wave soldering can be investigated.

Acknowledgement

The authors would like to thank the Ministry of Higher Education of Malaysia for the financial support for this research work and the PhD MyBrain15 scholarship programme. The technical supports of Shenzhen Kunqi Xinhua Technology Co. Ltd., China, and Cyntac Pte. Ltd., Singapore, are also greatly acknowledged.

References

1. Tan, W. and Ume, I.C. "Applications of lamination theory to study warpage across PWB and PWBA during convective reflow process", *IEEE Transactions on Components, Packaging and Manufacturing Technology*, **2**(2), pp. 217-223 (2012).

2. Cepeda-Rizo, J., Teneketges, N. and Yeh, H.-Y. "Characterization and modeling of printed wiring board warpage and its effect on LGA separable interconnects", *Transactions of ASME Journal of Electronic Packaging.*, **127**(2), pp. 178-184 (2005).

3. Ume, I.C., Martin, T. and Gatro, J.T. "Finite element analysis of PWB warpage due to the solder masking process", *IEEE Transactions on Components, Packaging, and Manufacturing Technology-Part A.*, **20**(3), pp. 295-306 (1997).

4. Lee, M. "Finite element modeling of printed circuit boards (PCBS) for structural analysis", *Circuit World*, **26**(3), pp. 24-29 (2000).

5. Hutapea, P., Grenestedt, J.L., Modi, M., Mello, M. and Frutschy, K. "Prediction of microelectronic substrate warpage using homogenized finite element models", *Microelectronic Engineering*, **83**(3), pp. 557-569 (2006).

6. Van Driel, W.D., Zhang, G.Q., Janssen, J.H.J., Ernst, L.J., Su, F., Chian, K.S. and Yi, S. "Prediction and verification of process induced warpage of electronic packages". *Microelectronics Reliability,* **43**(5), pp. 765-774 (2003).

7. Ding, H., Ume, I.C., Powell, R.E. and Hanna, C.R. "Parametric study of warpage in printed wiring board assemblies", *IEEE Transactions on Components and Packaging Technologies*, **28**(3), pp. 517-524 (2005).

8. Ying, M., Chia, Y.C., Mohtar, A., Yin, T.F. and Chuah, S.P. "Thermal induced warpage characterization for printed circuit boards with shadow moir system", *8th Electronics Packaging Technology Conference EPTC '06*, Singapore, pp. 265-270 (2006).

9. Wong, E.H. and Wong, C.K. "Approximate solutions for the stresses in the solder joints of a printed circuit board subjected to mechanical bending", *International Journal of Mechanical Sciences*, **51**(2), pp. 152-158 (2009).

10. Polsky, Y., Sutherlin, W. and Ume, I.C. "A comparison of PWB warpage Due to simulated infrared and wave soldering processes", *IEEE Transactions on Electronics Packaging Manufacturing*, **23**(3), pp. 191-199 (2000).

11. Johnson, A. "Lead-free soldering turns up the heat on PCB carriers", *Norplex Micarta, High performance thermoset composites*, pp. 1-3 (2008). http://www.norplex-micarta.com/whatsnew/Lead-Free%2010 1508.pdf

12. Hutapea, P. and Grenestedt, J.L. "Reducing warpage of printed circuit boards by using wavy traces", *Transactions of the ASME Journal of Electronic Packaging*, **126**, pp. 282-287 (2004).

13. Khor, C.Y., Abdullah, M.Z. and Che Ani, F. "Underfill process for two parallel plates and flip chip packaging", *International Communications in Heat and Mass Transfer*, **39**(8), pp. 1205-1212 (2012).

14. Balachandran, S. "Surfactant analysis of thin liquid film in the human trachea via application of volume of fluid (VOF)", *Fluid Dynamics, Computational Modeling and Applications*, pp. 449-462 (2012).

15. Yazdi, J., Sarkardeh, H., Azamathulla, H.M. and Ghani, A.A. "3D simulation of flow around a single spur dike with free-surface flow", *International Journal River Basin Management*, **8**(1), pp. 55-62 (2010).

16. Samarpana, K., Konapala, A. and Ramesh, D. "Computational investigation of free surface flow around a ship hull", *International Journal of Application or Innovation in Engineering* & *Management*, **2**(5), pp. 98-107 (2013).

17. Abdul Aziz, M.S., Abdullah, M.Z., Khor, C.Y. and Che Ani, F. "Influence of pin offset in PCB through-hole during wave soldering process: CFD modeling approach", *International Communications in Heat and Mass Transfer*, **48**, pp. 116-123 (2013).

18. Chen, G. and Chen, X. "Finite element analysis of flexBGA reliability", *Soldering and Surface Mount Technology*, **18**(2), pp. 46-53 (2006).

19. Shen, L., Wang, M., He, Y., Lam, T.F. and Jiang, Y.Q. "Reflow profile simulation by finite element method for a BGA package", *6th International Conference on Electronic Packaging Technology*, pp. 419-422 (2005).

20. Lau, C.-S., Abdullah, M.Z. and Che Ani, F. "Computational fluid dynamic and thermal analysis for BGA assembly during forced convection reflow soldering process", *Soldering and Surface Mount Technology*, **24**(2), pp. 77-91 (2012).

21. IPC-A-610E-2010, *Acceptability of Electronic Assemblies*, Ed. 3000 Lakeside Drive, Suite 309S, Bannockburn, IL, pp. 7-56 (2010).

22. Abdul Aziz, M.S., Abdullah, M.Z., Khor, C.Y., Jalar, A. and Che Ani, F. "CFD modeling of pin shape effects on capillary flow during wave soldering", *International Journal of Heat and Mass Transfer*, **72**, pp. 400-410 (2014).

23. Abdul Aziz, M.S., Abdullah, M.Z., Khor, C.Y., Fairuz, Z.M., Iqbal, A.M., Mazlan, M. and Mat Rasat, M.S. "Thermal fluid-structure interaction in the effects of pin-through-hole diameter during wave soldering", *Advances in Mechanical Engineering*, pp. 1-13 (2014).

Biographies

Mohd Sharizal Abdul Aziz received a bachelor degree in Mechanical Engineering and the MSc and PhD degrees in Computational Fluid Dynamics, focusing in Fluid-Structure Interaction (FSI), Advanced Packaging, and SMT from Universiti Sains Malaysia. Currently, he is a Lecturer at the School of Mechanical Engineering, Universiti Sains Malaysia. His research area are electronic packaging, thermofluids, heat transfer, soldering, Fluid Structure Interaction (FSI), and Computational Fluid Dynamics (CFD).

Mohd Zulkifly Abdullah is a Professor of Aerospace Engineering at Universiti Sains Malaysia since 2010. He obtained a bachelor degree in Mechanical Engineering from University of Swansea, U.K. His MSc and PhD degrees are from University of Strathclyde, U.K. He has numerous publications in international journals and conference proceedings. His areas of research are CFD, heat transfer, electronic packaging, electronic cooling, and porous medium combustion.

Khor Chu Yee received a bachelor degree in Mechanical Engineering and the MSc and PhD degrees in Computational Fluid Dynamics, specializing in electronics packaging from Universiti Sains Malaysia, Minden, Malaysia, in 2008, 2010, and 2013, respectively. He was a post-doctoral researcher at School of Mechanical Engineering, Universiti Sains Malaysia, 2014. Currently, he is a senior lecturer at the Faculty of Engineering Technology, Universiti Malaysia Perlis (UniMAP), Perlis, Malaysia. His current research interests include electronics packaging, fluid/structure interaction, fluid mechanics, dynamics, polymer rheology, heat, and mass transfers.

Ishak Abdul Azid received his BSc degree in Mechanical Engineering from Clarkson University, Potsdam, NY in 1992, MSc degree from University of Wales, Swansea, UK, in 1995, and PhD degree from University of Wales, Cardiff, UK, in 1999. He is currently a Professor of Mechanical Engineering at Universiti Kuala Lumpur (UniKL) Malaysian Spanish Institute. He has published more than 100 papers in journals and conferences. His research interests include micro electromechanical systems (MEMS), thermal management in electronic packaging, and application of artificial intelligence in optimization.

Azman Jalar is a Professor of Applied Metallurgy from the Faculty of Science and Technology and a principal research fellow in the Institute of Microengineering and Nanoelectronics (IMEN), Universiti Kebangsaan Malaysia. He received SmSn (BSc) in Materials Science from UKM and PhD degree in Metallurgy and Materials from the University of Birmingham, United Kingdom in 2001. He is the Head of Microelectronics Packaging and Materials (MIPAC) Research Group, and the current Deputy Director of (IMEN), UKM. His interest in microstructure-properties-performance of materials motivates him in the research area of electronics packaging. He has significantly contributed to solving many industrial-related semiconductor packaging problems through industry-driven research activities. Among his collaborators are on Semiconductor, Infineon, Freescale Semiconductor, AIC Semiconductor, Celestica, and Jabil Circuit. He has produced more than 200 publications in various referred journals and proceeding and held few patents. He is a member of the Institution of Electrical and Electronics Engineer (IEEE), Malaysian Association of Solid State Science and Technology (MASS), Electron Microscopy Society of Malaysia (EMSM) Akademi Sains Islam Malaysia (ASASI), and the Chairman of the Malaysian Electronics Packaging Research Society (EPRS).

Fakhrozi Che Ani is a Senior Advanced Technology Engineer (Asian Region) at Jabil Circuit Sdn Bhd, Penang , Malaysia (International Company based in US). His major role is in developing new technology content for Advanced Assembly & Printed Electronic. Electronics Packaging Research Society (EPRS), Malaysia, identify him as a Subject Matter Expert (SME). He has almost 20 years of experience in the SMT. He is a champion for many root cause findings and fundamental analysis pertaining to Surface Mount Technology. He obtained Bachelor Degree in Electrical and Electronic Engineering from University of Strathclyde, Scotland, UK and also obtained Master Degree (Research) from Institute of Microengineering and Nanoelectronics (IMEN). He is currently pursuing further study (PhD) in the field of materials science in Malaysia (Institute of Microengineering and Nanoelectronics, Universiti Kebangsaan Malaysia (IMEN)). On his Technical contributions, he has published more than 20 research papers to well-recognized international journal (Science Direct, Emerald, AJSE & IEEE). He has played major consultancy roles for many universities (Malaysia) seeking expertise in the field of SMT. His expertise is well-recognized by the universities in Malaysia, and he has supervised 2 master-degree students from University Science of Malaysia and has supervised more than 10 final year research students from various universities in Malaysia.